TÜBİTAK

Turkish Journal of Electrical Engineering & Computer Sciences

http://journals.tubitak.gov.tr/elektrik/

Research Article

Turk J Elec Eng & Comp Sci
(2013) 21: 1553 – 1566

doi:10.3906/elk-1108-8

Simulation of transient processes on overvoltage in electric transmission lines using ATP-EMTP

Ahmet NAYİR*
Department of Computer Programming, Fatih University, Büyükçekmece, İstanbul, Turkey

Received: 02.08.2011 • **Accepted:** 05.06.2012 • **Published Online:** 02.10.2013 • **Printed:** 28.10.2013

Abstract: In this paper, the mathematical modeling and simulation of electromagnetic transient processes is considered, which is of vital importance for examining the overvoltage phenomenon of power transmission systems. In the mathematical models of the AC power transmission systems that contain a power source, the power transformer, transmission line, and power autotransformer block are presented. The mathematical model of each system component is obtained based on the branch voltages, flux linkages, and branch voltages of the magnetic circuits individually. As for the simulation, an alternative transient program (ATP) environment is used to model the electric power system's elements. One of the power system's overvoltages occurs because of the fault and switching events. The usage of reactors at the sending and receiving ends of the line limits the overvoltages. The ATP has a powerful tool to simulate the transient events: specifically, the fault transients in the time domain. In order to test the simulation model's performance, the overvoltage measurements from a field test of a 500 kV electric transmission system is used. The simulation shows that the obtained results give satisfactory solutions to investigate the power system's overvoltage events. Selected results of the evaluation are presented.

Key words: Corona, electric transmission lines, mathematical model, overvoltage, simulation, skin effect

1. Introduction

Research of transients in electrical systems is one of the most important problems of power and electrical engineering. This problem covers a wide range of practical applications, such as the coordination of the overvoltages, overcurrents with their permissible values, or electromagnetic compatibility relay protection systems.

At the modern level of developed technologies of electrical power transmission, the problem of long-distance transmission can be solved with the use of super-high and ultra-high voltages, in both direct (500 kV, 600 kV, and 800 kV) and alternating (500 kV–750 kV, 1150 kV) forms. For power transmission with voltages of 500 kV, 750 kV, and 1150 kV, 98% percent of the faults result from the single-phase short circuits. In such a system, the failure rate for a 750 kV high-voltage line is assessed as 0.2 short circuits per 100 km per year [1]. More than 70% of the single-phase short circuits have an unstable character, i.e. they can be removed in the cycle of the short-term dead time with further reconstruction of the normal circuit. It is effective to recover the unsteady single-phase short circuits that arise on the transmission line using single-phase auto reclosing, from the view point of providing the minimal perturbations to the adjoining systems. Auto reclosing is the most important action, leading to an increasing of the reliability of the super-high voltage electrical power transmission. Both steady and unsteady single-phase faults in the alternating current electric transmission line (ETL) are suppressed by replacing the faulted phase with the reserve phase within 0.3–0.4 s [2].

*Correspondence: anayir@fatih.edu.tr

Power system transient analysis is usually performed using computer simulation packages like the Electromagnetic Transients Program (EMTP). Engineers and researchers who perform transient simulations typically spend only a small amount of their total project time actually running the simulations. For a better representation of the simulation blocks, a mathematical model of the most important components of a power system (lines, cables, transformers, rotating machines, arresters, and breakers) has the capability of representing the effects of the electromagnetic fields and losses [3].

Modern computer technology and bundled software, such as Mathcad, MATLAB, and EMTP, give an opportunity to prevent the difficulties that occur during the calculation of the unbalance in ETLs, and to test the speed and accuracy of the calculations [4].

In many situations, power system losses cannot be separated from electromagnetic fields. The skin effect and corona losses are 2 important phenomena. The skin effect is caused by the magnetic field constrained in the windings and produces frequency-dependent winding losses, and the corona losses are caused when the electric field exceeds the inception corona voltage. To represent the power system losses, elements such as the resistors, hysteresis cycle, combination of various types of circuit elements, frequency dependent models, and v-i characteristics of the corona can be used. The corona effect losses on the 500 kV transmission line have a very important influence on the temporary overvoltage damping [5,6].

One of the most important reasons for the occurrence of such regimes is the overvoltage and, accordingly, the ferroresonance conditions. Being one of the interesting phenomena, ferroresonance has been extensively investigated by the power engineering community. The first citations related to this phenomenon belong to the beginning of the 20th century [7]. Since then, a large number of papers have been published describing the phenomenon, proposing analytical methods or reporting experienced cases. Despite the extensive literature, ferroresonance still remains widely unknown and is feared by power systems operators, as it seems to occur randomly, possibly resulting in the catastrophic destruction of the plant's equipment. The occurrence of ferroresonance as a nonlinear phenomenon causes high enough overvoltages and results in major hazards for power transmission networks. Some interesting practical examples of ferroresonance hazards in a high-voltage transmission system were presented in [8,9].

In this study, the blocks for the power source, power transformer, transmission line, and power autotransformer are developed in the Alternative Transient Program (ATP)-EMTP. The skin effects and influence of the corona discharge are considered in the model. For the simulation, a 500 kV ETL system is modeled to investigate the sending- and receiving-end overvoltages. To validate the model's accuracy, a single-phase ground fault is created and compared with the actual data.

2. Calculation method

The proposed power transmission system is shown in Figure 1. The mathematical model of each system component is obtained based on the branch voltages, flux linkages, and branches voltages of magnetic circuits individually. Electric power system generations consist of a set of synchronous and asynchronous generators from the electric power stations and the connection lines between them. During electric transmission transient analysis, power system generators are often represented in a simplified way.

The system, which contains a group of power stations connected by high- and ultra-high voltage lines, can be replaced by an equivalent electromotive force applied before the equivalent impedance.

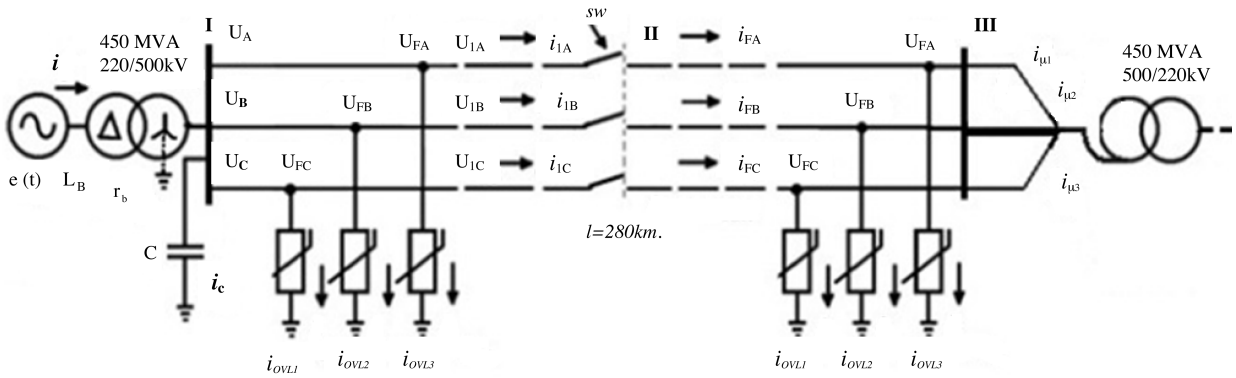

Figure 1. Calculation scheme for the computer modeling.

Time-dependent equations for the calculation of the voltages u and i and the initial node I are as follows:

$$\begin{gathered}\frac{d_{i_1}}{d_t} = L_b^{-1}\left[e(t) - r_b i_1 - U_e\right], \\ \frac{di_{r_1}}{dt} = L_{r_1}^{-1} \cdot U_1 \\ i = i_e + i_{r_1} \\ U_e = (z + z_n) \cdot (i_1 - i_{r_1}) - V_q, \\ \frac{du}{dt} = C^{-1} \cdot ic,\end{gathered} \tag{1}$$

where the power supply inductance L_b, resistance r_b, and total capacitance C have the form of a 3×3 matrix, according to the type of the power transformer connected to the system. Moreover, $e(t)$ is the power supply voltage; u and i are the instantaneous values of the voltage and current through the power supply, respectively; I is the node currents; and i_c is the total capacitance current, defined as:

$$e(t) = \begin{bmatrix} e_A \\ e_B \\ e_C \end{bmatrix} = E_{\max} \cdot \begin{bmatrix} \sin(\omega t + \phi) \\ \sin(\omega t + 2\pi/3 + \phi) \\ \sin(\omega t + 4\pi/3 + \phi) \end{bmatrix};$$

Here, φ is the angle of the supply voltage when the switch is on and E_{max} is the maximum generated voltage of the supply.

Below, i_1 and i_{r1} are the matrices of the current of the general and longitudinal windings, and L_b and r_b are the quadratic matrices of the inductance of the common and longitudinal windings. Moreover, matrix L_T contains the reactor inductance of the neutral L_g:

$$L_b = \begin{bmatrix} L_T + \frac{2}{3}L_g & -\frac{1}{3}L_g & -\frac{1}{3}L_g \\ -\frac{1}{3}L_g & L_T + \frac{2}{3}L_g & -\frac{1}{3}L_g \\ -\frac{1}{3}L_g & -\frac{1}{3}L_g & L_T + \frac{2}{3}L_g \end{bmatrix} \quad r_b = \begin{bmatrix} r_T + \frac{2}{3}r_g & -\frac{1}{3}r_g & -\frac{1}{3}r_g \\ -\frac{1}{3}r_g & r_T + \frac{2}{3}r_g & -\frac{1}{3}r_g \\ -\frac{1}{3}r_g & -\frac{1}{3}r_g & r_T + \frac{2}{3}r_g \end{bmatrix}$$

$$i_1 = \begin{bmatrix} i_A \\ i_B \\ i_C \end{bmatrix}; \quad i_{r1} = \begin{bmatrix} i_{rA} \\ i_{rB} \\ i_{rC} \end{bmatrix}; \quad i_e = \begin{bmatrix} i_A \\ i_B \\ i_C \end{bmatrix}; \quad i_c = \begin{bmatrix} i_{cA} \\ i_{cB} \\ i_{cC} \end{bmatrix}; U_e = \begin{bmatrix} U_A \\ U_B \\ U_C \end{bmatrix}; \quad V_q = \begin{bmatrix} V_{q_A} \\ V_{q_B} \\ V_{q_C} \end{bmatrix},$$

where V_q is the voltage value of the ETL.

The conditions in the intermediate substation require the expression of the magnetic flux in the transformer by the following equation:

$$\frac{d}{dt}\begin{bmatrix} \Psi_A \\ \Psi_B \\ \Psi_C \end{bmatrix} = \begin{bmatrix} -1 - L_1F(\Psi_A) + L_{b1}L_{b2}^{-1} & -\frac{1}{3}L_1L_2^{-1} & -\frac{1}{3}L_1L_2^{-1} \\ -\frac{1}{3}L_1L_2^{-1} & -1 - L_1F(\Psi_A) + L_{b1}L_{b2}^{-1}\frac{1}{3} & -\frac{1}{3}L_1L_2^{-1} \\ -\frac{1}{3}L_1L_2^{-1} & -\frac{1}{3}L_1L_2^{-1} & -1 - L_{B1}F(\Psi_A) + L_{b1}L_{b2}^{-1} \end{bmatrix} \begin{bmatrix} U_{e_A} \\ U_{e_B} \\ U_{e_C} \end{bmatrix}.$$

The currents in the primary winding are given as follows [10,11]:

$$\frac{di_{eA}}{dt} = L_{b1}^{-1}\left(\frac{d\Psi_A}{dt} - U_{eA}\right),$$

$$\frac{di_{eB}}{dt} = L_{b1}^{-1}\left(\frac{d\Psi_B}{dt} - U_{eB}\right),$$

$$\frac{di_{eC}}{dt} = L_{b1}^{-1}\left(\frac{d\Psi_C}{dt} - U_{eC}\right). \tag{2}$$

The magnetizing currents can be given in the following form [10,11]:

$$F(\psi) = a + \ nb\ \psi^{n-1} + mc\psi^{m-1}; m > n,$$

$$\phi(\psi_A) = a + nb\phi_A^{n-1} + mc\phi_A^{m-1},$$

$$\phi(\psi_B) = a + nb\phi_B^{n-1} + mc\phi_B^{m-1},$$

$$\phi(\psi_C) = a + nb\phi_C^{n-1} + mc\phi_C^{m-1}, \tag{3}$$

where ψ is the magnetic flux; i_1 and i_2 are the primer and secondary currents; i_μ is the magnetic current; L_1, L_2 and r_1, r_2 are the resistances and inductances and the common and transformer windings of the autotransformer, respectively; and a, b, c, n, and m are functions as equivalents that approximately depend on the magnetic flux of the magnetic current. The mathematical model of the AC power transmission block 'power source - power transformer - transmission line - power autotransformer' is presented below. The mathematical model of the system is created on a coordinate basis of the voltages of the electric circuit branches, flux linkages, and magnetic voltages of the magnetic circuit branches using separate models of each element.

2.1. Mathematical model of the ETL

In the proposed mathematical model of the 3-phase transmission line, the traveling wave method is implemented to improve the model's performance, which is modeled in the ATP environment.

The approximation, by the use of the finite-difference method, is presented in Figure 2.

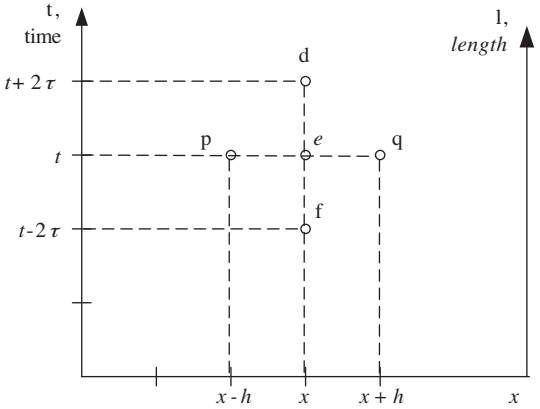

Figure 2. The finite-difference approximation approach for the transmission line equation.

According to Figure 2, the following finite-difference approach is used: the approximate solution of the equations for each of the 3 nodes, using the characteristics method, is performed through the construction of the grid of characteristics and the calculation of the voltages and currents on the grid points, as presented in [10,11].

If the forward and reverse characteristics go through points p and q, and d is their point of intersection, then it is possible to calculate the values of the voltage and current by changing the differentials to differences in the differential relations.

We select a line segment l as a calculation step, and thereafter we apply the second-order finite-difference method.

For the mathematical expression of node II, we will use the well-known equations of the ETL, which take into account the skin effect and the influence of the corona discharge as follows [10,11].

Various developed methods and algorithms for the numerical analysis of the wave-induced processes in complex electrical circuits have found a wide spectrum of applications [10–12]. Mathematical models taking into account the skin effect and wires of the corona are overlapped in these developments with the calculation formulae of the ETL.

Equations of the multiwire line, taking into account the corona and skin effect in the ground and wires, have the following matrix form:

$$-\frac{\partial u}{\partial x} = L_0 \frac{\partial i}{\partial t} + f\left(\frac{\partial i}{\partial t}, i\right)$$

$$-\frac{\partial i}{\partial x} = C_0 \frac{\partial u}{\partial t} + \phi\left(\frac{\partial u}{\partial t}, u\right). \tag{4}$$

Here, L_0 and C_0 are the matrices of the characteristic and the mutual geometrical inductances and capacities of the ETL; u and i are the column matrices of the voltages and currents, respectively; $f\left(\frac{\partial i}{\partial t}, i\right)$ is a function taking into account the influence of the skin effect; and $\phi\left(\frac{\partial u}{\partial t}, u\right)$ is a function taking into account the influence of the wires of the corona.

The matrix coefficients for the 3-phase transmission with an alternate phase in Eq. (4) have the following

form:

$$L_0 = \begin{vmatrix} L_{11} & L_{12} & L_{13} \\ L_{21} & L_{22} & L_{23} \\ L_{31} & L_{32} & L_{33} \end{vmatrix}, \quad C_0 = \begin{vmatrix} C_{11} & C_{12} & C_{13} \\ C_{21} & C_{22} & C_{23} \\ C_{31} & C_{32} & C_{33} \end{vmatrix},$$

where the matrix elements are the values of the self and mutual geometrical inductance and capacitance:

$$L_{nn} = \frac{\mu_0}{2\pi} ln \frac{2h_n}{r_n},$$

$$L_{nk} = \frac{\mu_0}{2\pi} ln \frac{2D_{nk}}{d_{nk}}.$$

L_{nn} are the eigenvalues of the inductance and L_{nk} are the mutual inductances of the line, and

$$\frac{\mathcal{C}F}{km} C_{nn} = \left(0.018.ln \frac{2h_n}{r_n}\right)^{-1},$$

$$\frac{\mathcal{C}F}{km} C_{nk} = \left(0.018.ln \frac{2D_{nk}}{d_{nk}}\right)^{-1}.$$

Here, $\mu_0 = 4\pi.10^{-7}\,(H/m)\,\mu_0 = 4\pi\ 10^{-7}$ (H/m) is the magnetic inductivity of the cable material, h_n is the average height of the nth wire bracket; r_n is the radius of the nth wire; d_{nk} is the distance between the nth and kth wires; D_{nk} is the distance between the nth wire and the mirror projection of the kth wire; and m is the quantity of the wires in TL, n = 1, 2, 3; k = 1, 2, 3.

The geometrical sizes between the wires and their mirror projections for the 3-phase ETL are shown in Figure 3.

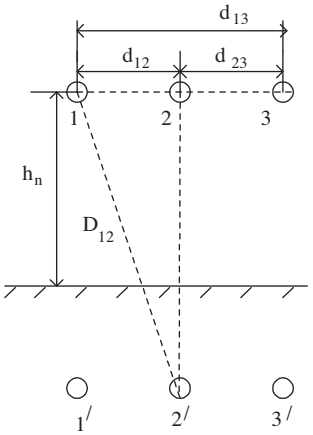

Figure 3. Geometrical sizes between the wires and their mirror projections for the 3-phase ETL.

The equations are solved in the domain, limited by the straight lines x = 0, x = l, and t = 0, and are open in direction t. The following formulas have been obtained based on Figure 2 by Nayir [13–15]:

$$U_d - -U_p + z(i_d - -i_p) + h[z\phi_e\left(\frac{\partial u}{\partial t}, u_e\right) + fe\left(\frac{\partial i}{\partial t}, i_e\right)] + 0(h^2) = 0,$$

$$-U_d + U_q + z(i_d - -i_p) + h[z\phi_e\left(\frac{\partial u}{\partial t}, u_e\right) + fe\left(\frac{\partial i}{\partial t}, i_e\right)] + 0(h^2) = 0, \tag{5}$$

where $z = (L_0/C_0)^{0,5}$ is the impedance of the line without the losses and h and τ are the spatial and time variables. The relation between these variables is equal to the traverse speed of the electromagnetic wave across the lossless line and it determines the calculation of $= (L_0/C_0)^{0,5}h$. The remainder of the term of the approximated Eq. (5) is:

$$(h^2) = -\frac{h^2}{2}\left(L_0\frac{\partial}{\partial t}f_e - \frac{\partial}{\partial x}f_e + C_0\frac{\partial}{\partial t}\varphi_e - \frac{\partial}{\partial t}\varphi_e\right),$$

Here, u_d, u_p, u_q, u_e, i_d, i_p, i_q, and i_e are the voltages and currents in the points of the considered domain of the solution of Eq. (5), with coordinates (x,t), $(x - h,\ t - \tau), (x + h,\ t - \tau)$, and $(x,\ t - \tau)$, respectively. The calculation formulas for the computation of the column matrices of the voltages and currents u_d and i_d in the multiwire ETL with coordinates (x,t) are given in Eq. (6).

Based on Eq. (5) and by the use of the proposed model, which considers the skin effect and different models of the corona [11], the following calculation formulas for the computation of voltages and currents in the intermediate points of the ETL are obtained:

$$\left.\begin{array}{l}(1+\sigma)\,u_d + (z+z_s)\,i_d = u_p + zi_p + \sigma u_f + \theta_1 + \theta_2 \\ -(1+\sigma)\,u_d + (z+z_s)\,i_d = -u_q + zi_q - \sigma u_f + \theta_1 - \theta_2\end{array}\right\}, \tag{6}$$

or by another form:

$$u_d = 0,5(1+\sigma)^{-1}\left[U_p + U_q + z\left(i_p - i_q\right) + 2\sigma\left(\pm u_3\right) + 2\theta_2\right]$$

$$i_d = 0,5(Z+Z_s)^{-1}\left[U_p - U_q + Z\left(i_p - i_q\right) + 2\theta_1\right].$$

Here, *ud*, *uq*, *ip*, and *iq* are the column k-dimensional matrices of the known voltages and currents in points p and q of the ETL with coordinates $p(x - h,\ t - \tau), q(x + h,\ t - \tau)$. The column k-dimensional matrix is:

$$\theta_1 = \begin{bmatrix}\theta_{1_1}\\ \theta_{1_2}\\ \theta_{1_3}\end{bmatrix}, \quad \theta_1 = Z_1\sum_{k=1}^{3}\chi_k i_k$$

Here, Z_1 and χ_k are the matrix coefficients and i_k is the current. The column k-dimensional matrix is: $\theta_2 = hZ\sum_{k=1}^{3} G_k U_{fck}$,

U_{fck} is the known voltage in point f, h is the calculation step on the distance, Z is the square matrix of the wave resistances of the line without the losses, and Gk is the coefficients, given in [10].

The symbol σ in Eq. (6) is a k $\times$ k coefficient matrix. Here, the σ is equal to hGZ and G is a determinable diagonal matrix. The system model for the calculation is given in Figure 1, where $z = \left(L_0 C_0^{-1}\right)^{0,5}$ is the wave resistance of the line without the loss, and the variables and coefficients for the 3-phase line have the following form:

$$u_d = \begin{bmatrix}u_{dA}\\ u_{dB}\\ u_{dC}\end{bmatrix}, i_d = \begin{bmatrix}i_{dA}\\ i_{dB}\\ i_{dC}\end{bmatrix}, u_p = \begin{bmatrix}u_{pA}\\ u_{pB}\\ u_{pC}\end{bmatrix}, i_p = \begin{bmatrix}i_{pA}\\ i_{pB}\\ i_{pC}\end{bmatrix}, u_q = \begin{bmatrix}u_{qA}\\ u_{qB}\\ u_{qC}\end{bmatrix}, i_q = \begin{bmatrix}i_{qA}\\ i_{qB}\\ i_{qC}\end{bmatrix}, z_s = \begin{bmatrix}z_{AA} & z_{AB} & z_{AC}\\ z_{BA} & z_{BB} & z_{BC}\\ z_{CA} & z_{CB} & z_{CC}\end{bmatrix},$$

$$u_f = \begin{bmatrix} u_{f_1} \\ u_{f_2} \\ u_{f_3} \end{bmatrix} \quad \sigma = hz \sum_{k=1}^{3} \sigma_k,$$

The inaccuracy of the calculation of the line in Eq. (6) is determined by the Runge principle [16], separately for the current and the voltage:

$$\begin{aligned} \varepsilon_i &= \frac{i\,(0,5h) - i\,(h)}{n^2 - 1}; \\ \varepsilon_u &= \frac{u\,(0,5h) - u\,(h)}{n^2 - 1} \end{aligned},$$

where $\mathcal{E}_i$ and $\mathcal{E}_u$ are the inaccuracies in the calculation of the current and the voltage; *i(0,5)*, $i(h)$, *u(0,5h)*, and $u(h)$ are the values of the calculated currents and voltages with the length step of *0,5h*; and h and n is the order of the approximation inaccuracy [10].

After some transformations, the calculation of the inaccuracy of the current has the form:

$$\varepsilon_i = -\frac{1}{12z}\left[\left(\frac{z_s}{z} - \sigma\right) hL_0\omega I + \sigma u_f\right].$$

The relative inaccuracy of the current calculation is:

$$\varepsilon_i^* = \frac{\sigma z - z_s}{12z^2} hL_0\omega - \frac{\sigma u_f}{12zI}.$$

The relative inaccuracy of the voltage calculation after similar transformations has the form:

$$\varepsilon_u^* = \frac{\sigma z - z_s}{12z^2} hC_0\omega - \frac{\sigma u_f}{12zI}.$$

In node III of the model, one can write the equation for:

$$\frac{d\psi}{dt} = u_T - u_0,$$

where ψ is the instantaneous value of the magnetic linkage:

$$\psi = \begin{bmatrix} \psi_A \\ \psi_B \\ \psi_C \end{bmatrix}.$$

According to the calculation scheme (Figure 1), u_T and u_0 are defined as follows:

$$u_T = \begin{bmatrix} u_{FA} \\ u_{FB} \\ u_{FC} \end{bmatrix},$$

$$u_0 = \frac{1}{3}(u_{FA} + u_{FB} + u_{FC}).$$

The conditions in the intermediate substation require the expression of the magnetic flux in the transformer by the following equation.

$$\frac{d}{dt}\begin{bmatrix}\psi_A\\ \psi_B\\ \psi_C\end{bmatrix}=\begin{bmatrix}1+L_1\phi(\psi_A)-L_1L_2^{-1}\frac{1}{3} & -\frac{1}{3}L_1L_2^{-1} & -\frac{1}{3}L_1L_2^{-1}\\ -\frac{1}{3}L_1L_2^{-1} & 1+L_1\phi(\psi_B)-L_1L_2^{-1}\frac{1}{3} & -\frac{1}{3}L_1L_2^{-1}\\ -\frac{1}{3}L_1L_2^{-1} & -\frac{1}{3}L_1L_2^{-1} & 1+L_1\phi(\psi_C)-L_1L_2^{-1}\frac{1}{3}\end{bmatrix}\begin{bmatrix}U_{SA}\\ U_{SB}\\ U_{SC}\end{bmatrix}$$

The currents in the primary winding are as follows:

$$\begin{aligned}\frac{di_{SA}}{dt}&=L_1^{-1}\left(U_{SA}-\frac{d\psi_A}{dt}\right),\\ \frac{di_{SB}}{dt}&=L_1^{-1}\left(U_{SB}-\frac{d\psi_B}{dt}\right),\\ \frac{di_{SC}}{dt}&=L_1^{-1}\left(U_{SC}-\frac{d\psi_C}{dt}\right),\end{aligned}\tag{7}$$

and the magnetizing currents have the following form [10]:

$$\begin{aligned}i_{\mu A}&=a\psi_A+b\psi_A^n+c\psi_A^m,\\ i_{\mu B}&=a\psi_B+b\psi_B^n+c\psi_B^m,\\ i_{\mu C}&=a\psi_C+b\psi_C^n+c\psi_C^m.\end{aligned}\tag{8}$$

The magnetization curve can be introduced into the model in the form of $i_{\mu A}=f_A(\psi)$, $i_{\mu B}=f_B(\psi)$, $i_{\mu C}=f_C(\psi)$, using the analytic approximation carried out for the A,B, and C phases considering the core dimension for the different phases, where:

$$i_{\mu A}=a\psi_A+b\psi_A^9+c\psi_A^{11}$$

$$i_{\mu B}=a\psi_B+b\psi_B^9+c\psi_B^{11}$$

$$i_{\mu C}=a\psi_C+b\psi_C^9+c\psi_C^{11}$$

$$\frac{d_{i_{\mu A}}}{dt}=\phi(\psi_A)\frac{d\psi_A}{dt};$$

$$\frac{d_{i_{\mu B}}}{dt}=\phi(\psi_B)\frac{d\psi_B}{dt};$$

$$\frac{d_{i_{\mu C}}}{dt}=\phi(\psi_C)\frac{d\psi_C}{dt};.$$

The ETL is modeled using [17] taking into account the corona effect, and using [18] without taking into account the corona effect. The overvoltage limiter (OVL) is modeled as in [19,20], where:

$$\phi(\psi_A)=a+9b\phi_A^8+11c\phi_A^{10},$$

$$\phi(\psi_B) = a + 9b\phi_B^8 + 11c\phi_B^{10},$$
$$\phi(\psi_C) = a + 9b\phi_C^8 + 11c\phi_C^{10},$$

where a = 0.15, b = 0,18, and c = 0.67,

$$\phi_{ref} = \frac{\sqrt{2}U_n}{\sqrt{3}\cdot 314}\ I_{ref} = k_F \cdot I_0\ U_{ref} = U_n \cdot I.$$

Here, I_0 = peak value for the transformer's current, K_F = coefficient, and k_F = 1.6 / 1.7 for the autotransformer.

3. ATP-EMTP model

The EMTP was used for the simulation of the overvoltage phenomenon. The program works well; however, other methods are more suitable for specific problems [4,21–23]. The model used in the ATP-EMTP overvoltage investigation is shown in Figure 4.

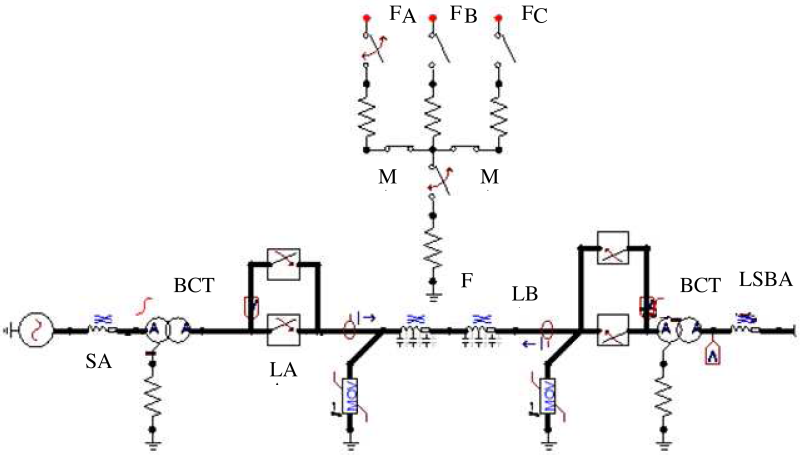

Figure 4. The ATP model of the system.

The model of the electric transmission in the form 'power source - transmission line - autotransformer' is implemented using the ATP. The parameters are taken from a real transmission line, which are as shown in the Table.

Table. Parameters of the modeled transmission network.

System element	Parameter	
Double-circuit line	Length, l	280 km
	R_{I+}	0.0139 Ω/m
	R_{I0}	0.3869 Ω/m
	L_+	0.185
	L_0	1.4027
	C_+	0.0282
	C_0	0.0108

One of the good estimation methods to investigate the overvoltage and accordingly the ferroresonance phenomenon in the multiwire system is to use the ATP computer program, allowing us transients simulations.

The simulations are done using the ATP computer program for the calculation of the transient processes on overvoltage in the electric transmission lines. Analysis of the overvoltage processes is performed for an ETL with a 280 km length.

4. Simulation results and discussion

Simulation of the block transients based on the developed mathematical model was conducted. The transient waveforms of the block switching with the initial conditions are presented in Figures 5–9.

In order to verify the adequacy of the proposed ETL model, a comparison method was employed. The simulation results of the transmission block 'power source - transformer - transmission line - autotransformer' obtained using the proposed models and the models built into the ATP (3-phase source, 3-phase transformer, 3-phase line, and 3-phase autotransformer) were compared. A simulation of the same processes was conducted. The quantitative similarity of the currents and voltages was observed. The quantitative differences can be explained by the differences in the methods of the calculation of the parameters of the electric system's elements.

All of the wave forms in the article were measured for 0.4 s. A fault with phase A occurred at 0.1 s. The voltage value decreased at phase A after 0.1 s, and an increase in phases C and B was seen. The voltage surge in the sending end of the ETL was stopped after the reactor (OVL) was connected to the circuit. The voltage variation in the sending end versus the time of the ETL with 500 kV is given in Figure 5. As can be seen from Figure 5, the voltage arose to more than a 500 kV_{peak} value. This voltage was needed when the loss at the ETL was considered.

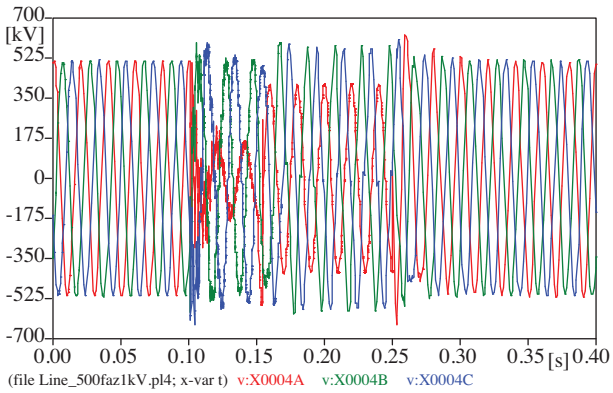

Figure 5. Voltage value of phases A, B, and C of the 500 kV line (sending).

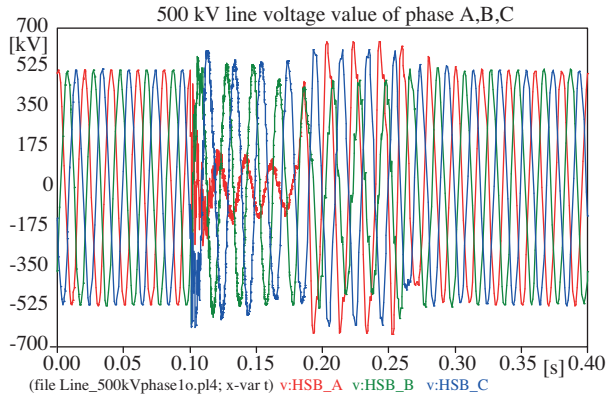

Figure 6. Voltage value of phases A, B, and C of the 500 kV line (receiving).

Although the fault occurred in the middle of the ETL, the sending-end and receiving-end overvoltage waveforms were different from each other.

The voltage surge that occurred in the autotransformer was obtained as in Figure 7. The autotransformer's voltage value in its 220 kV side stayed at approximately 220 kV, which was expected.

As is seen from the current wave form of the 500 kV line in Figure 8, the current values increased quite a lot after the fault. When the reactor switch was on, the current wave form returned to normal.

As a result of the computer simulations, the curves of the currents with the 3-phase OVL are presented in Figure 9.

The wave form of the current flowing from the reactor is seen in Figure 9. Before the breakdown, no flow was observed. The reactor was switched on after the fault happened, at 0.1 s, and the value of the current

increased. When the fifth harmonic was seen, the reactors were connected to a circuit at both ends of the line. Many calculations were made in order to control the applicability of this technique. It is possible to protect the system against overvoltage with this method.

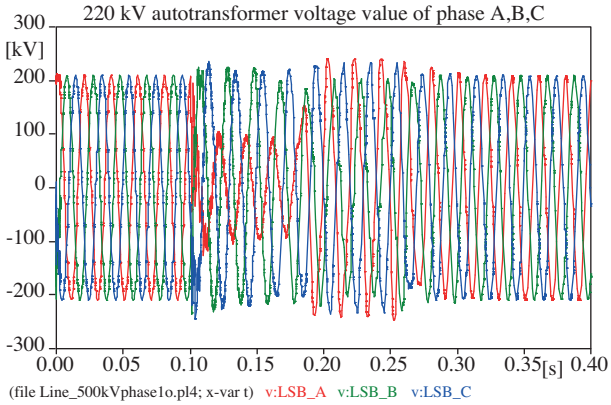

Figure 7. Voltage value of phases A, B, and C of the 220 kV autotransformer.

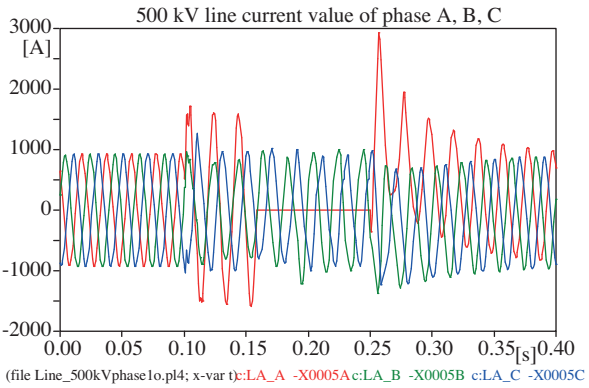

Figure 8. Current value of phases A, B, and C of the 500 kV line.

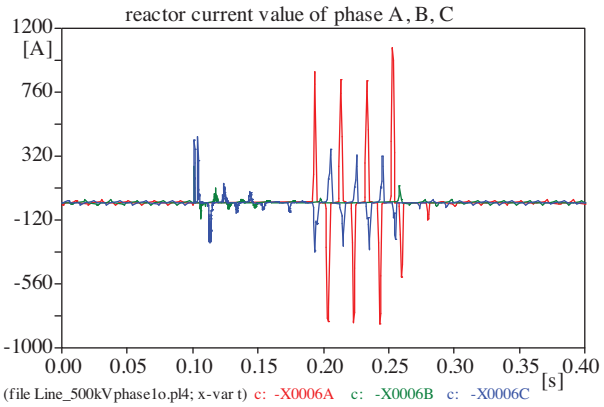

Figure 9. Current value of phases A, B, and C of the OVL.

The latest technological achievements in the field of power system relay communications create new possibilities for fault location approaches [24].

It is important to verify the simulation results with the real overvoltage phenomenon. However, it is almost impossible to set up such a system in laboratory conditions to test the overvoltage events. Therefore, the best way to verify the simulation results is with the recorded data from a real power system. That is why simulation tools are required for such research. The simulation results can be compared with the actual fault data, but one should keep in mind that each fault has circumstantial parameters and should be evaluated separately as such. When compared with the actual fault data given in [25], it is possible to observe that our results are in agreement with the actual fault data. Although the simulation results and actual data are not exactly the same, the sufficient similarity between them is satisfied to prove the adequacy of the proposed model.

5. Conclusions

The key factors that affect the overvoltage processes have been analyzed and discussed. An analytical analysis was carried out using a time domain simulation with the ATP version of the EMTP. The simulation results were almost identical when compared with the field measurements of the 500 kV systems.

The proposed mathematical model of the ETL is suitable for the analysis of the transient processes during the switching and faulting regimes. It was confirmed by the investigation of the transients and modes of the power autotransformer, transformer, and transmission line as separate elements. The main advantages of the proposed model are its universality and possibility of modification.

In this article, the overvoltage case that has damaging effects on transmission lines was modeled with the help of the ATP-EMTP package program in a 3-phase system, and a general approach was obtained. The wave fluctuations that occurred in the system were analyzed and the results were evaluated. The analysis showed that components with a high frequency occurred when the overvoltage was formed on the transmission lines. They were high-frequency components out of 50 Hz. It is clear that changes in the voltage and frequency would be destructive for the system.

As for future work, all symmetric and asymmetric faults can be considered. Moreover, a preestimation of the overvoltages caused by the faults can be done using intelligent systems. The fault location can be automatically detected based on the fault information obtained from the ETL and the resulting signal sent to the control center via GPS technologies [23].

Acknowledgments

The author would like to make an acknowledgment of the Polish Government; the Ministry of Education of Turkey; Fatih University, İstanbul, Turkey; and the Wroclaw University of Technology Institute of Electrical Power Engineering, Wroclaw, Poland.

References

[1] F.M. Gatta, F. Iliceto, "Analyses of some operation problems of half-wave length power transmission lines", IEEE/CIGRE Africon'92 Conference, Swaziland, pp. 59–64, 1992.

[2] G. Samorodov, T. Krasilnikova, V. Dikoy, S. Zilberman, R. Iatsenko, "Nonconventional reliable AC transmission systems for power delivery at long and very long distance", Proceedings of the IEEE Transmission and Distribution Conference, Vol. 2, pp. 982–987, 2002.

[3] F.M. Gatta, F. Iliceto, "Analyses of some operation problems of half-wave length power transmission lines", IEEE/CIGRE Africon'92 Conference, Swaziland, pp. 59–64, 1992.

[4] G. Samorodov, T. Krasilnikova, V. Dikoy, S. Zilberman, R. Iatsenko, "Nonconventional reliable AC transmission systems for power delivery at long and very long distance", Proceedings of the IEEE Transmission and Distribution Conference, Vol. 2, pp. 982–987, 2002.

[5] J.A. Martinez, J. Mahseredjian, R.A. Walling, "Parameter determination: procedures for modeling system transients", IEEE Power and Energy Magazine, Vol. 3, pp. 16–28, 2005.

[6] M.V. Escudero, I. Dudurych, M. Redfem, "Understanding ferroresonance", Proceedings of the 39th International Universities Power Engineering Conference, Vol. 3, pp. 1262–1266, 2004.

[7] T.T. Quoc, S.L. Du, D.P. Van, N.N. Khac, L.T. Dinh, "Temporary overvoltages in the Vietnam 500 kV transmission line", IEEE 8th International Conference on Transmission & Distribution Construction, Operation & Live-Line Maintenance Proceedings, pp. 225–230, 1998.

[8] CIGRE WG 33.02, Guidelines for Representation of Network Elements When Calculating Transients, CIGRE Brochure 39, 1990.

[9] P. Boucherot, "Existence de deux regimes en ferroresonance", Revue Française de lElectricité, Vol. 8, pp. 827–828, 1920 (in French).

[10] T. Tsao, C. Ning, "Analysis of ferroresonant overvoltages at Maanshan nuclear power station in Taiwan", IEEE Transactions on Power Delivery, Vol. 21, pp. 1006–1012, 2006.

[11] D.A. Jacobson, D.R. Swatek, R.W. Mazur, "Mitigating potential transformer ferroresonance in a 230 kV converter station", IEEE Proceedings of the Transmission and Distribution Conference, pp. 359–365, 1997.

[12] Y.V. Dimitriyev, A.M. Hashimov, A. Nayir, "Elektrik iletim hatlarında oluşan gerilimlerin modelleri", Baku, Elm, 2002 (in Turkish).

[13] A.M. Gashimov, E.V. Dmitriyev, I.R. Pivchik, "Numerical analysis of wave processes in electric networks", Novosibirsk, Science, 2003 (in Russian).

[14] P. Stakhiv, O. Hoholyuk, "Simulation of electrical transmission transient processes using MATLAB/Simulink", Proceedings of the International Symposium on Modern Electric Power Systems, pp. 447–452, 2006.

[15] A. Nayir, "Sistemlerarası elektrik iletiminde kaza açılmalarından oluşan gerilimlerin modelleri", Autoreferat, Baku, Elm, 2001 (in Turkish).

[16] A. Nayir, A.M. Haşimov, Y.V. Dimitriyev, "Elektrik iletim hatlarında kaza açılmalarından oluşan gerilimlerin modelleri", Baku, Elm, 2002 (in Turkish).

[17] S.İ. Hasanov, A.M. Haşimov, A. Nayir, Y.V. Dimitriyev, I.R. Pivçik, "Ferrorezonans ve aşırı gerilimlerden korunmak için matematiksel model", Elektrik-Elektronik ve Bilgisayar Mühendisliği 10. Ulusal Kongresi, pp. 193–196, 2003 (in Turkish).

[18] G.I. Marchuk, Methods of Numerical Mathematics, 2nd ed., Berlin, Springer-Verlag, 1982.

[19] C.M. Juvarly, E.V. Dmitriyev, A.M. Gashimov, B.M. Sadikhov, "Calculation formulas for equations of electric transmission lines taking into account surface effect and corona", Technical Electrodynamics, pp. 85–92, 1991.

[20] A.M. Gashimov, E.V. Dmitriyev, I.R. Pivchik, "Numerical analysis of wave processes in electric networks", Novosibirsk, Science, 2003.

[21] C.M. Juvarly, E.V. Dmitriyev, A.M. Gashimov, V.M. Maksimov, B.M. Sadikhov, "Application of the spline interpolation for modelling of the overvoltages limiters", Doklady - Azerbaijan NAS, Vol. 12, pp. 24–27, 1986.

[22] P. Pinceti, M. Giannettoni, "A simplified model for zinc oxide surge arresters", IEEE Transactions on Power Delivery, Vol. 14, pp. 393–397, 1999.

[23] J. Izykowski, M. Bozek, "Distance relaying algorithm for double - circuit transmission line with compensation for reactance effect under standard availability of measurements", Turkish Journal of Electrical Engineering & Computer Sciences, Vol. 16, pp. 217–227, 2008.

[24] S.P. Ang, "Ferroresonance simulation studies of transmission systems", PhD, The University of Manchester, 2010.

[25] P. Dawidowski, J. Izykowski, A. Nayir, "Non-iterative algorithm of analytical synchronization of two-end measurements for transmission line parameters estimation and fault location", 7th International Conference on Electrical and Electronics Engineering, pp. 76–79, 2011.

[26] M.M. Saha, J. Izykowski, E. Rosolowski, Fault Location on Power Networks, London, Springer-Verlag, 2010.

[27] A.M. Haşimov, A. Nayir, Y.V. Dimitriyev, "Protection of energy transmission lines from the ferroresonance overvoltages with high harmonics", Yıldız Teknik Üniversitesi Dergisi, pp. 19–24, 2001 (in Turkish).